

Adaptation-and-Collision Detection Scheme for Safe Physical Human-Robot Interaction

Chang Nho Cho, Young-Loul Kim, Jae-Bok Song

School of Mechanical Engineering

Korea University

Seoul, Korea

lsdfzz@korea.ac.kr, kimloul@korea.ac.kr, jbsong@korea.ac.kr

Abstract— Human-robot collisions are unavoidable during a human-robot interaction. Thus, a number of collision detection algorithms have been proposed to ensure human safety during such an occasion. However, collision detection algorithms are usually model-based, requiring an accurate model of the robot. The errors in the model can lead to the malfunction of the algorithms. In this study, we propose an adaptation and collision detection scheme to improve the sensitivity of the collision detection algorithm. Performing adaptation prior to collision detection will effectively minimize the model uncertainty of the robot. This minimization will allow sensitive, reliable collision detection. By using torque filtering, adaptation and collision detection can be done without the need for the acceleration estimation. The performance of the proposed scheme is demonstrated by various experiments.

Keywords— *Adaptive control; Collision detection; Collision safety;*

I. INTRODUCTION

Service robots often share the same workspace with humans to perform cooperative tasks, so physical interactions including collisions between humans and robots are inevitable. To ensure collision safety, several solutions employing variable stiffness actuators (VSA) [1], joint stiffness reduction mechanism [2] and vision system [3] were proposed, with their own advantages and disadvantages.

On the other hand, several researchers proposed collision detection algorithms, which allow a robot to detect a collision [4, 5]. Once a collision is detected, the robot can perform an appropriate reaction to ensure human safety. Using generalized momentum, the need of acceleration estimation was effectively removed [6]. However, while these collision detection algorithms can effectively detect a collision, they are all model-based and thus, they require an accurate model of the robot. However, such a model is hard to obtain, and it is bound to change as the robot grasp an object.

Many robust or adaptive control strategies have been proposed to deal with the model uncertainty of robots. The precise model of a robot can be extracted without the need for acceleration by employing indirect adaptive control [7]. This control method monitors the difference between the predicted and the actual torques to perform parameter identification. The need for acceleration is effectively removed by the filtering of

torques. It was shown that torque filtering can be used for simple FDI (Fault Detection and Isolation) [8]. However, the feasibility of torque filtering on collision detection was never discussed.

In this study, we expand the use of indirect adaptive control and torque filtering to collision detection. An on-line adaptation process before the execution of the collision detection algorithm can be used to accurately extract the robot model. This process is to be repeated upon payload variation to update the robot model. With the accurate model of the robot, a collision can be effectively detected by monitoring the difference between the predicted and the actual torques.

The remainder of this paper is organized as follows. In section 2, the model identification scheme will be introduced. In section 3, the proposed collision detection algorithm is presented, and in section 4, the proposed scheme is overviewed. Section 5 presents the experimental results, and section 6 presents our conclusion.

II. MODEL IDENTIFICATION

A. Torque filtering

Many collision detection algorithms are model-based. It was shown that today's CAD (Computer-Aided Design) models can provide accurate models of robots [9]. Therefore, the CAD model itself should be accurate. However, robots often handle a payload, which would induce a change in the robot model. This change cannot be reflected by the CAD model. For these reasons, adaptation is needed to update the given robot model.

In this study, indirect adaptive control is employed to extract the model of a robot from its joint torques. In general, the joint torque can be calculated by using acceleration estimation, which often contains noise and is inaccurate. However, the need for acceleration estimation can be effectively removed by using torque filtering.

The dynamics of a robot can be expressed by,

$$M(q)\ddot{q} + C(q, \dot{q})\dot{q} + g(q) + F_v\dot{q} + F_c \operatorname{sgn}(\dot{q}) = \tau \quad (1)$$

where q is the joint angle, $M(q)$ is the inertia matrix, $C(q, \dot{q})$ is the centrifugal and Coriolis terms, $g(q)$ is the gravitational load, F_v is the viscous friction coefficient, F_c is the column friction coefficient, τ is the actuator torques and $\text{sgn}(\cdot)$ is the sign function to extract the sign of a variable. For adaptation purposes, a regressor matrix is often employed, which can be expressed as:

$$\tau = W(q, \dot{q}, \ddot{q})\theta \quad (2)$$

where $W(q, \dot{q}, \ddot{q})$ is the regressor matrix, which is a function of q , \dot{q} , and \ddot{q} , and θ is the matrix of unknown, constant robot parameters. Note that both Eq. (1) and (2) require the use of acceleration estimation. To deal with this problem, we can define a filtered version of the torques [10]:

$$\tau_f = f * \tau \quad (3)$$

where $*$ is the convolution operator and f is the impulse response of a proper, stable filter. Note that a low-pass filter is used in this study. It should be noted that convolution shows the following property:

$$f * \dot{x} = \dot{f} * x \quad (4)$$

Note that the acceleration term in Eq. (1) can be expressed as the convolution of the velocity and the time-derivative of the impulse response by using Eq. (4). Then, by using Eq. (1), (2) and (4), Eq. (3) can be expanded as:

$$\begin{aligned} \tau_f = & \dot{f} * (M(q)\dot{q}) + f(0)M(q)\dot{q} - fM(q(0))\dot{q}(0) + \\ & f * (-\dot{M}(q)\dot{q} + C(q, \dot{q})\dot{q} + g(q) + F_v\dot{q} + F_c \text{sgn}(\dot{q})) \end{aligned} \quad (5)$$

and $\tau_f = W_f(q, \dot{q})\theta$

where $W_f(q, \dot{q})$ is the filtered regressor matrix. Note that these two equations do not require the estimation of acceleration. Now we are motivated to use this for parameter identification.

B. Model Identification

The exact model of a robot is often unknown, so model uncertainty is inevitable. In the presence of such uncertainty, Eq. (6) can be expressed as:

$$\hat{\tau}_f = W_f(q, \dot{q})\hat{\theta} \quad (7)$$

where $\hat{\tau}_f$ is the estimated filtered torques and $\hat{\theta}$ is the estimated robot parameters. From Eq. (6) and (7), the error ε between the actual and the estimated filtered torque is given by

$$\varepsilon = \tau_f - \hat{\tau}_f = W_f(q, \dot{q})\tilde{\theta} \quad (8)$$

where $\tilde{\theta}$ is the error in the estimated parameter, which is given by

$$\tilde{\theta} = \theta - \hat{\theta} \quad (9)$$

The estimated filtered torque, $\hat{\tau}_f$, can be found by using Eq. (7), and the actual filtered joint torque, τ_f , can be found by filtering the joint torque sensor signal using Eq. (3). From Eq. (8), we can set up an adaptation law as follows:

$$\dot{\hat{\theta}} = P W_f^T \varepsilon \quad (10)$$

where P is the diagonal, positive definite adaptation gain matrix.

There are many ways of updating the gain matrix [11]. In this study, the least-squares method is employed. This method extracts the maximum amount of parameter information even when the given motion is not under constant excitation [10]. Furthermore, it enables a smooth convergence of the parameters. Thus, the use of the least-squares method would allow the robot to obtain its model while following a general trajectory.

III. COLLISION DETECTION ALGORITHM

Torque filtering described in the previous section can be used to perform collision detection without acceleration estimation. When a robot collides with an object, an external torque is induced at each joint of the robot, as shown in Fig. 1.

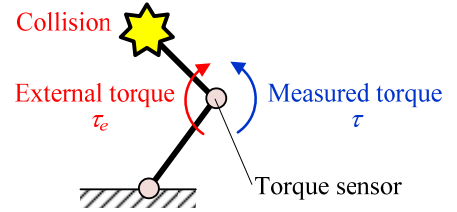


Figure 1. Collision of 2-DOF robot arm.

In such a case, Eq. (1) can be rewritten as

$$M(q)\ddot{q} + C(q, \dot{q})\dot{q} + g(q) + F_v\dot{q} + F_c \text{sgn}(\dot{q}) = \tau - \tau_e \quad (11)$$

where τ_e is the external torque. This also can be expressed in the filtered regressor form:

$$\tau_f = W_f(q, \dot{q})\theta + \tau_{ef} \quad (12)$$

where τ_{ef} is the filtered version of the external torque. Thus, collision detection becomes a matter of extracting the external torque from Eq. (12), and the extraction can be done by

comparing the estimated filtered joint torque and the actual filtered joint torque.

Note that the basic principle of collision detection is the same as adaptation. We monitor the difference between the measured torque and the predicted torque. However, with the model uncertainty minimized, the difference between the two filtered torques must be caused by a collision.

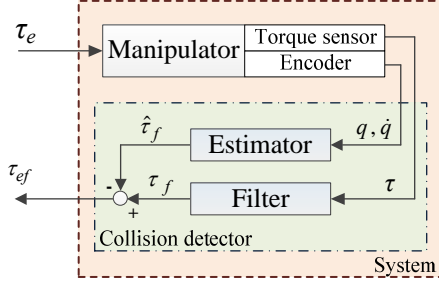


Figure 2. Collision detection algorithm.

The block diagram of the proposed collision detection algorithm is shown in Fig. 2, where “estimator” and “filter” correspond to Eq. (7) and Eq. (3), respectively. As shown in Fig. 2, the filtered external torque can be estimated by

$$\tau_f - \hat{\tau}_f = W_f(q, \dot{q})\theta + \tau_{ef} - W_f(q, \dot{q})\hat{\theta} \approx \tau_{ef} \quad (13)$$

given that $\theta \approx \hat{\theta}$.

Ideally, the estimated external torque, τ_{ef} , remains zero during a normal operation, but when the external torque due to a collision is applied, it rises abruptly, as can be seen in Eq. (13). Thus, by comparing it to the pre-determined threshold, a collision can be detected. Therefore, the collision index F_i can be given as

$$F_i = \begin{cases} 1 & \text{if } |\tau_{ef,i}| > \text{threshold} \\ 0 & \text{if } |\tau_{ef,i}| \leq \text{threshold} \end{cases} \quad (i = 1, \dots, n) \quad (14)$$

where i is the joint number. Normally, the threshold must be set higher than the sensor noise and the error in the estimated external torque due to the model uncertainty of the robot to avoid any possible malfunctions. However, in this study, collision detection is performed after the adaptation process, and thus, the collision detection threshold can be minimized.

Note from Eq. (13) and (14) that the external torques of each joint can be evaluated individually, which means the collision signal will be an $n \times 1$ vector. Thus, for an n -DOF robot arm, if a collision occurs at joint m , where $m \leq n$, the estimated external torques for only joint 1 to m would increase while the others remain constant; hence, the location of the collision can be estimated. Furthermore, the collision direction can be obtained from the sign of the external torque, so that the robot can perform an effective reaction against the collision.

Once a collision is detected, the robot must perform an appropriate reaction to minimize the impact force. Several reaction strategies are proposed [6]. These strategies can be combined with the proposed collision detection algorithm since they also use the external torque. In this study, a simple position-based strategy was adopted, and the robot was programmed to withdraw from the collision location as quick as possible to minimize the impact.

IV. ADAPTATION-AND-COLLISION DETECTION SCHEME

In this study, an adaptation and collision detection scheme is proposed. Thus, the robot needs to know when to complete the adaptation phase and enter the normal operation/collision detection phase, during which the parameters are kept constant. In this study, the following threshold-based termination condition is used:

$$|\tau_{ef,i}| \leq \beta \quad (i = 1, \dots, n) \quad \text{for } t_0 < t < t_0 + T \quad (15)$$

where t is the time, t_0 is the start time of the adaptation process, and T and β are the pre-defined values of the period and the desired collision detection threshold, respectively. During the adaptation phase, as there is no collision, τ_{ef} becomes zero as the model uncertainty decreases. Thus, if τ_{ef} at each joint is within the desired boundary β for the pre-defined period T , we may conclude that the estimated parameters are accurate enough to be used for collision detection. This process ensures that the robot enters the collision detection phase if and only if the desired, safe collision detection threshold can be achieved. To further prevent any possible malfunctions, a value slightly greater than β is recommended as the collision detection threshold in the actual collision detection phase. Such thresholds can be experimentally determined, considering the robot's noise level.

During an operation, a robot may have to change its end-effector tools or pick up an object. This will certainly change the model of the robot, preventing sensitive collision detection. In such a case, the robot can simply perform the adaptation again, as shown in Fig. 3. It would be reasonable to assume that the robot knows when it changes its end-effector tools or picks up an object.

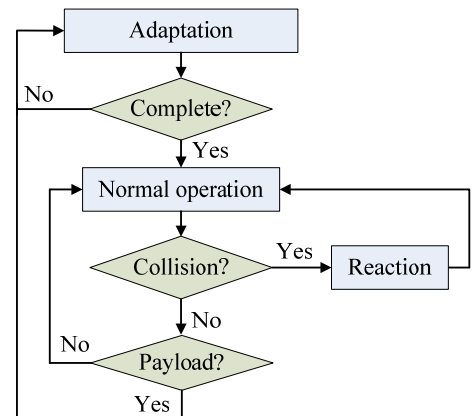


Figure 3. Overview of proposed procedure.

V. EXPERIMENTS

A. Experimental setup

To demonstrate the performance of the proposed collision detection procedure, several experiments were conducted using a 2 DOF robot arm. The experimental set up is shown in Fig. 4. As can be seen from Fig. 4, a socket for a 1 kg mass was installed at the end of link 2 to simulate payload variation. Also, a joint torque sensor developed and built in our lab was installed at each joint of the robot. A PC with RTOS (Real-Time Operating System) from National Instrument was used to control the robot at 1 kHz.

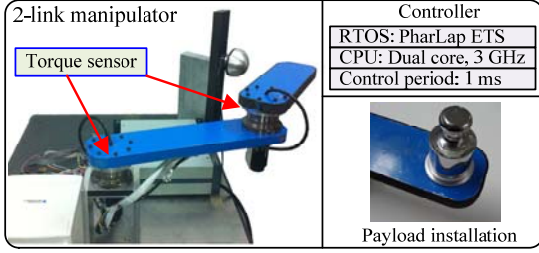


Figure 4. Experimental setup.

To perform torque filtering, a filter was required, as can be seen from Eq. (3). In this study, a low-pass filter was adopted to effectively suppress the noise from the sensors. A low-pass filter can be described as

$$F(s) = \frac{b}{s + a} \quad (16)$$

where a is the cutoff frequency and b is the filter gain.

There is a tradeoff between the noise reduction performance and the response time. In this study, both a and b were set to 10. This value was experimentally determined, so that the algorithm can quickly detect a collision.

The overall scheme of the experiment is as follows: First, since all the estimated parameters were set to zero initially, the robot performs adaptation. Once the adaptation process is completed, a collision will be applied to the robot when it is moving. Then, the robot was given a 1 kg payload, which triggers another adaptation process. After that, another collision is applied, to see if the robot can detect a collision after a change in its payload. Throughout the experiment, a 5-th order polynomial trajectory was used, which commands the robot to move joints 1 and 2 by $\pm 30^\circ$ and $\pm 60^\circ$, respectively. The maximum speed of each joint is 100 °/s for joint 1 and 50 °/s for joint 2.

For the experiment, the desired threshold for the termination condition, β , was set to 0.1 Nm while the actual collision detection threshold was set to 0.15 Nm. The required duration, T , was set to 5 s, which was chosen so that the parameters of the robot would have sufficient time to converge. On the other hand, the adaptive gains were set as $P = \text{diag}\{8, 4, 4, 0.5, 0.5, 0.5, 0.5\}$. These gains were experimentally selected based on the fact that the parameters with more influence on the joint torques need higher gains.

B. Robot model

The regressor form of the robot is required for model identification. The dynamics of a robot can be expressed as [12]:

$$\begin{aligned} \begin{bmatrix} \tau_1 \\ \tau_2 \end{bmatrix} &= \begin{bmatrix} a_1 + 2a_2c_2 & a_3 + a_2c_2 \\ a_3 + a_2c_2 & a_3 \end{bmatrix} \begin{bmatrix} \ddot{q}_1 \\ \ddot{q}_2 \end{bmatrix} \\ &+ \begin{bmatrix} -a_2s_2\dot{q}_2 & -a_2s_2(\dot{q}_1 + \dot{q}_2) \\ a_2s_2\dot{q}_1 & 0 \end{bmatrix} \begin{bmatrix} \dot{q}_1 \\ \dot{q}_2 \end{bmatrix} \\ &+ \begin{bmatrix} a_4c_1 + a_5c_{12} \\ a_5c_{12} \end{bmatrix} + \begin{bmatrix} a_6\dot{q}_1 \\ a_7\dot{q}_2 \end{bmatrix} + \begin{bmatrix} a_8 & 0 \\ 0 & a_9 \end{bmatrix} \begin{bmatrix} \text{sgn}(\dot{q}_1) \\ \text{sgn}(\dot{q}_2) \end{bmatrix} \end{aligned} \quad (17)$$

where

$$\begin{aligned} a_1 &= I_1 + m_1l_{c1}^2 + I_2 + m_2(l_1^2 + l_{c2}^2) \\ a_2 &= m_2l_1l_{c2} \\ a_3 &= I_2 + m_2l_{c2}^2 \\ a_4 &= (m_1l_{c1} + m_2l_1)g \\ a_5 &= m_2l_{c2}g \\ a_6 &= F_{v2} \\ a_7 &= F_{v1} \\ a_8 &= F_{c1} \\ a_9 &= F_{c2} \end{aligned} \quad (18)$$

and I_i is the moment of inertia for link i , m_i is the mass of link i , l_i is the length of link i , and l_{ci} is the distance to the center of mass for link i , F_{vi} and F_{ci} are the viscous and Coulomb friction coefficients for joint i , respectively, and c_i and s_i represent the cosine and sine of the angle of joint i .

Because the robot used for the experiments moves in the horizontal plane, the terms a_4 and a_5 can be omitted. For adaptation, Eq. (17) can be re-arranged into the filtered regressor matrix as shown in Eq. (6), and

$$\theta = [a_1 \ a_2 \ a_3 \ a_6 \ a_7 \ a_8 \ a_9]^T \quad (19)$$

C. Collision detection results

To verify the performance of the proposed collision detection algorithm, the estimated external torque τ_{ef} using both the estimated parameters and the CAD model are presented. As stated in previous sections, the estimated external torque should remain zero during normal operations, but increase rapidly upon a collision. However, due to the errors in the robot model, this value will fluctuate, as shown in the experimental results. For actual collision detection, the external torque estimated with the estimated parameters is used.

The results are represented in Fig. 5. For easier understanding, the whole experimental procedure is divided into 5 sections as follows:

TABLE I. SECTIONS OF EXPERIMENT

Section	Description
A	Adaptation
B	Collision detection
C	1 kg weight installation
D	Adaptation
E	Collision detection

As shown from the plots, throughout the experiment, the errors were decreased dramatically by using the identified parameters. Therefore, one can use a lower collision detection threshold to improve the sensitivity of the algorithm. Of course, using a more accurate CAD model would also minimize the error; however, as stated in previous sections, merely using a more accurate CAD model cannot compensate the error due to payload variations, as can be seen from sections D and E.

From sections A and B in Fig. 5, it can be verified that by using the estimated parameters, the threshold can be greatly reduced, and the collision, which took place at 10 s, is successfully detected. Also, it should be noted that it only took 5.2 s for the adaptation phase to complete. Figure 5(b) shows that for joint 2, τ_{ef} using the CAD model shows a good result. This is due to the fact that joint 2 does not experience much torque, and the error would increase upon the addition of the payload.

Sections D and E shows the estimated external torque upon the addition of the 1 kg mass. It triggered the second adaptation phase, which took about 5.3 s to complete. As can be seen from the results, the estimated external torque using the CAD model shows a much larger error with the 1 kg payload, but the one with the estimated parameters stays within the threshold. Furthermore, joint 2, which previously showed a good result using the CAD model, exhibits much greater error upon the payload change.

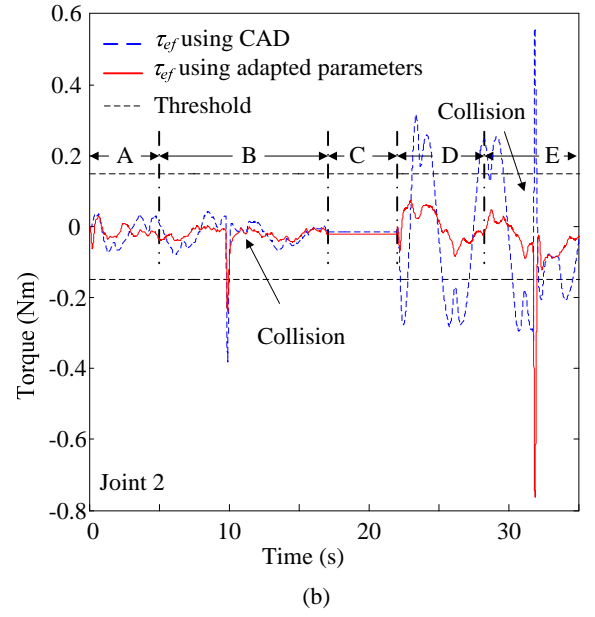
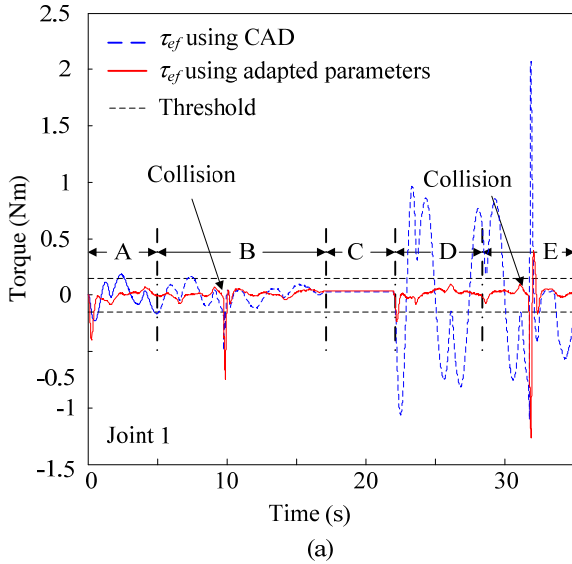


Figure 5. Error in (a) joint 1, and (b) joint 2.

D. Model identification results

The results of two model identification phases are separately plotted in Fig. 6 and 7. Note that the values have not fully converged to their exact values. However, doing so would take too much time, and as verified from other results, with these estimated parameters, we can achieve the desired collision detection performance.

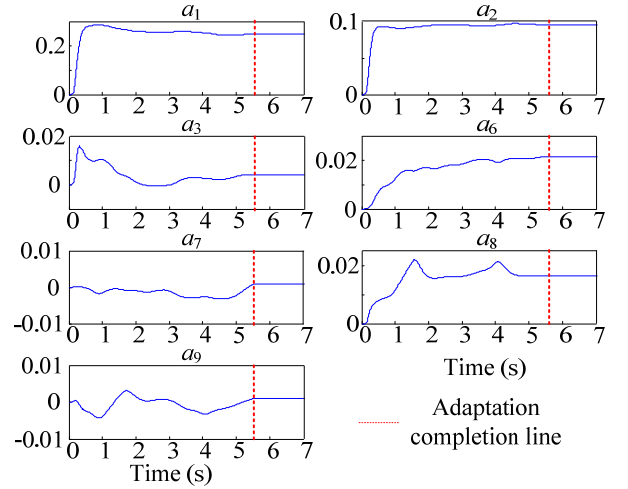


Figure 6. Model identification results 1.

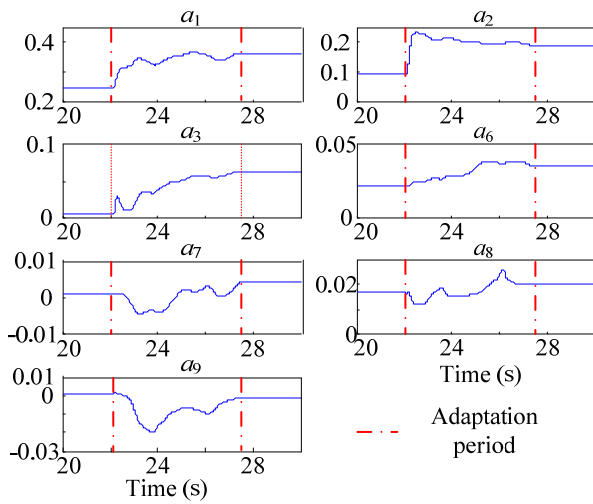


Figure 7. Model identification results 2.

VI. CONCLUSION

In this study, the limitations of conventional model based collision detection algorithms were discussed, and a novel adaptation-and-collision detection scheme was proposed to improve the performance of the collision detection algorithm. Using torque filtering, an accurate model of a robot can be obtained without the need for acceleration estimation, and with the same technique, an acceleration-free collision detector was developed. This procedure can be applied to any robot with joint torque sensing capability. The following conclusions were drawn from this study:

1. An acceleration-free collision detector was developed using torque filtering. This algorithm can effectively detect the presence, location, direction and magnitude of a collision.
2. The proposed adaptation-and-collision detection scheme enables reliable and sensitive collision detection even with model uncertainty. Furthermore, it allows robots to detect collisions upon a payload change.
3. Although collision safety cannot be guaranteed during the model identification phase, this phase is completed in about 5 s; thus, this gap in collision safety should not be a serious drawback under most circumstances.

ACKNOWLEDGMENT

This work was supported by the Human Resources Development Program for Convergence Robot Specialists (NIPA-2012-H1502-12-1002) and by the MKE under the Industrial Foundation Technology Development Program supervised by the KEIT (No. 10038660).

REFERENCES

- [1] B. S. Kim, J. J. Park, and J. B. Song, "A serial-type dual actuator unit with planetary gear train: basic design and applications," *IEEE/ASME Transactions on Mechatronics*, vol. 15, pp. 108-116, February 2010.

- [2] J. J. Park and J. B. Song, "A nonlinear stiffness safe joint mechanism design for human robot interaction," *ASME Journal of Mechanical Design*, vol. 132, pp. 061005-1-8, 2010.
- [3] S. Morikawa, T. Senoo, A. Namiki, and M. Ishikawa, "Realtime collision avoidance using a robot manipulator with light-weight small high-speed vision system," *Proc. of the IEEE International Conference on Robotics and Automation*, pp. 794-799, Roma, April 10-14, 2007.
- [4] S. Takakura, T. Murakami, and K. Ohnishi, "An approach to collision detection and recovery motion in industrial robot," *Proc. of 15th Annual Conference of IEEE Industrial Electronics Society*, pp. 421-426, Boston, MA, Nov. 6-10, 1989.
- [5] M. Bouattour, M. Chadli, M. CHaabane, and A. E. Hajjaji, "Design of robust fault detection observer for Takagi-Sugeno models using the descriptor approach," *International Journal of Control, Automation, and system*, vol. 9, pp. 973-979, 2011.
- [6] A. D. Luca, A. Albu-Schaffer, S. Haddadin, and G. Hirzinger, "Collision detection and safe reaction with the DLR-III lightweight manipulator arm," *Proc. of the IEEE International Conference on Intelligent Robotics and Systems*, pp. 1623-1630, Beijing, Oct. 9-15, 2006.
- [7] J. J. Craig, P. Hsu, and S. S. Sastry, "Adaptive control of mechanical manipulators," *The International Journal of Robotics Research*, vol. 6, pp. 16-28, 1987.
- [8] W. E. Dixon, I. D. Walker, D. M. Dawson, and J. P. Hartranft, "Fault detection for robot manipulators with parametric uncertainty: a prediction-error-based approach," *IEEE Transactions on Robotics and Automation*, vol. 16, pp. 689-699, 2000.
- [9] A. Albu-Schaffer, and G. Hirzinger, "Parameter identification and passivity based joint control for a 7 DOF torque controlled light weight robot," *Proc. of the IEEE International Conference on Robotics and Automation*, pp. 2852-2858, Seoul, May 21-26, 2001.
- [10] F. L. Lewis, D. M. Dawson, and C. T. Abdallah, *Robot Manipulator Control: Theory and Practice*, Marcel Dekker, Inc., New York, 2003.
- [11] F. J. Vijverstra, "Direct Indirect and Composite Adaptive Control of Robot Manipulators," WFW Rapport 92.076, Eindhoven University of Technology, 1992.
- [12] L. Sciavicco, and B. Siciliano, *Modeling and Control of Robot Manipulators*, Springer, UK, 2000.